



# Innovation and Research for Space Elevators

**JOHN M. KNAPMAN** International Space Elevator Consortium

**Email** john.knapman@isec.org

**DOI** <https://doi.org/10.59332/jbis-076-07-0238>

Progress continues on suitable materials for constructing the tether of a space elevator. Graphene super laminate is the most promising, and manufacturers are already producing significant quantities of graphene. Work is also continuing on a multi-stage space elevator, supported dynamically using magnetic levitation; the advantage is that it can be built with weaker materials, or even with materials that are already available today. The far end of a space elevator offers exciting opportunities to launch interplanetary spacecraft frequently with little or no fuel and with gentle rides at low cost. The node at geosynchronous altitude can accommodate unlimited mass and offers many commercial and scientific opportunities such as astronomy, communications and space-based solar power.

**Keywords:** Little Fuel, Gentle Rides, Available Materials, Interplanetary

## 1 MATERIALS

There has been steady progress on the number one requirement for building a space elevator, namely the availability of a material that is light, long and strong enough to produce a tether capable of supporting its own weight under the Earth's gravitational field between the surface and a height of 100,000 km. Graphene super laminate is the most promising candidate [1]. Not only does it have the right properties, typically a tensile strength of 130 GPa and mass density of 2,300 kg/m<sup>3</sup>, but it has many other useful properties that have prompted companies to manufacture and market substantial quantities of polycrystalline graphene. Although they are not long enough for a space elevator, they are able to add strength to carbon composite materials and are already being incorporated into such products as motor cars and golf equipment as well as into building materials such as concrete. Moreover, the electrical properties are substantially superior to those of copper, and they promise a new era of light-weight and efficient electric motors and more efficient electric power transmission.

Graphene super laminate consists of multiple sheets, each one atom thick. Each sheet consists of a single crystal, effectively a single molecule. The sheets are held together by van der Waals forces, but there are opportunities to create stronger bonds by using the fourth covalent bond of the carbon atoms, since only three are used in the 2-D hexagonal structure of a single crystal. These crystals are created by depositing carbon vapour on a copper film.

Another promising material is hexagonal boron nitride (hBN), which also forms 2-D sheets. It has the necessary strength and light weight, typically 105 GPa and 2,100 kg/m<sup>3</sup>. Thus the specific strength is  $105 \times 10^9 / 2,100 = 50 \times 10^6$ , i.e., 50 MYuri, whereas graphene has a specific strength of 130 ×

$10^9 / 2300 = 56.5 \times 10^6$ , i.e., 56.5MYuri. (The Yuri is the preferred unit of specific strength, named after Yuri Artsutanov, a pioneer of space elevators; one Yuri equates to one Pa/kg.m<sup>-3</sup>.) The minimum specific strength required is 38 MYuri [2]. A team in South Korea has reported a successful technique using a liquid metal substrate to create sheets of hBN, which has the advantage that the single crystal of hBN can be removed from the substrate without damage to the crystal, an essential step towards making a 2-D material that can be used in building a space elevator [3].

Before the recent progress in 2-D materials, carbon nanotubes were the favoured construction material for a space elevator. They are known as 1-D materials and need to be formed into fibre bundles of consistent quality over substantial lengths. The specific strength of a single nanotube is higher than that of graphene or hBN at 154 MYuri (200 GPa and 1,300 kg/m<sup>3</sup>). Practical strengths for a short bundle of a dozen nanotubes have been achieved of 42 MYuri (76 GPa and 1,800 kg/m<sup>3</sup>).[4]

## 2 A MULTI-STAGE SPACE ELEVATOR

Another way of approaching the construction of a space elevator is to consider building up from the Earth's surface. The idea is to make the requirements on the tether material less stringent in the expectation that a suitable material in the necessary quantities will be available sooner.

The Thoth Tower is one method of building upwards [5]. It relies on a stack of inflatable cushions that can reach a height of 20 km. Another method is to use the idea of the Launch Loop, also known as the Lofstrom Loop [6]. This was proposed as a way of supporting a structure up to 80 km above the Earth's surface by means of an iron core travelling at 14 km/s using magnetic levitation inside an evacuated tube to eliminate almost all the friction. The motion of the iron core round the

curves in the tube and the curves of the Earth's surface creates a centrifugal force that counteracts gravity. Furthermore, a little of the momentum of the iron core can be transferred to a spacecraft. A Launch Loop 2,000 km long is enough to accelerate a spacecraft at  $50 \text{ m/s}^2$  ( $\approx 5 \text{ g}$ ) to orbital velocity (8 km/s) relying solely on electrical power.

A development of the Launch Loop has been proposed called the Space Cable that is much smaller [7]. It is designed to replace the role of a first-stage rocket, launching spacecraft with a maximum mass of 90 tonnes to a velocity of 1.6 km/s at a height of 50 km. It consists of evacuated tubes forming an arch 150 km long. Inside the tubes, instead of an iron core, a stream of discrete magnetic objects called bolts travel at 2.0 km/s. Having discrete objects makes it easier to deal with the variations in their velocity and spacing that occur at different altitudes and during launching or construction.

The interesting application of this idea to the space elevator is to construct a tower, effectively a vertical loop rather than a curved arch. To support a platform 100 km above the Earth's surface the bolts must travel at 2.3 km/s at the bottom, slowing to 2.07 km/s at the top. There they enter a semi-circular structure called an ambit, which turns the bolts around using a combination of permanent magnets and electromagnets so that they return to the Earth's surface where they are again turned around by another ambit. As the bolts travel round the ambit they exert a strong centrifugal force upwards that is enough to support the weight of the platform, about 150 tonnes, and the weight of the tubes below, which is about 1,000 tonnes. This is an example of a dynamically supported structure.

The main tether of the space elevator is anchored to this platform, which is itself anchored to the Earth by the tubes through which the bolts travel. This anchorage is essential for transmitting the Coriolis force along the tether. The Coriolis force slowly accelerates climbers on the tether in the orbital direction so that they reach the orbital velocity of 3.1 km/s at the geosynchronous altitude (GEO) and even faster at the end.

The first advantage of the tower formed by the vertical loop is that the tether is not subject to wind forces and other atmospheric phenomena. Instead, the vertical loop deals with them using a technique called *active curvature control*. The tubes bend with the wind in such a manner that the bolts travelling round these bends exert a centrifugal force that opposes the wind. A proof of stability has been published in Ref. [7]. Recent work has focused on simulating this stabilization process at the detailed level of calculating the currents needed in each elec-

tromagnetic coil.[8] This work is still ongoing.

The dynamically supported platform only relieves the tether of part of its load. To allow a space elevator to be built with material that may be available sooner, a more radical idea is to build several stages, of which the platform at 100 km altitude is the first [9]. For example, a two-stage space elevator can be built with material having a specific strength of 11 MYuri, compared to the 38 MYuri needed to build a conventional space elevator. 11 MYuri is only three times the specific strength of existing commercially available material such as Torayca carbon fibre yarn (3.9 MYuri, 7 GPa and  $1,790 \text{ kg/m}^3$ ).

In the two-stage space elevator, the second stage is at 6,000 km. It supports the tether below it, the mass of which is 2,400 tonnes. The tether above the second stage has a mass of 4,200 tonnes. It is able to support its own weight at the higher altitudes because of the reduced gravity there. The tether reaches to an altitude of 88,000 km, somewhat less than the 100,000 km altitude in the standard model of space elevators.

Above the Earth's atmosphere, no evacuated tubes are required. Instead, the bolts travel in a stream in the vacuum of space. Calculations and simulations have shown that the ascending bolts can use the descending bolts emerging from the second stage to steer themselves towards the opening through which they must enter into another ambit to turn them around and send them back down towards the first stage. The centrifugal force this creates is enough to support the 2,400 tonne tether below plus the weight of the climbers on it. Similarly, the descending bolts use the ascending bolts to guide them to the opening at the first stage that takes them into the tubes down to the earth's surface, where they enter the lower ambit which turns them around so that they ascend again in a continuous loop.

Using more than two stages permits a space elevator tether to be made of progressively weaker materials. Five stages, the highest being at 14,600 km, would be enough for the tether to be made of materials already available commercially. There is a trade-off here. The multi-stage space elevator is more complex than the standard model, but it uses existing materials and technologies, albeit in novel ways. Some components have been built towards the construction of a small-scale prototype (see Fig. 1 and Fig. 2), and work is in progress to demonstrate stability and reliability.

The first step is to build a four-metre-high prototype in a workshop (Fig. 3) as a step towards a mile-high (1.6 km) tower (Fig. 4). Preliminary construction in the Andaman Sea off

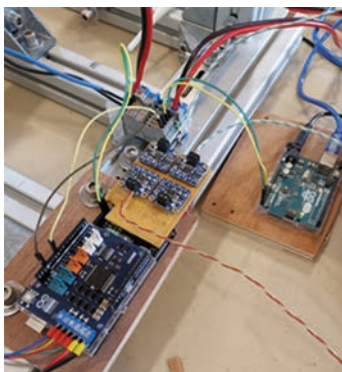


Fig.1 Components under test.



Fig.2 Test rig in the vacuum chamber.

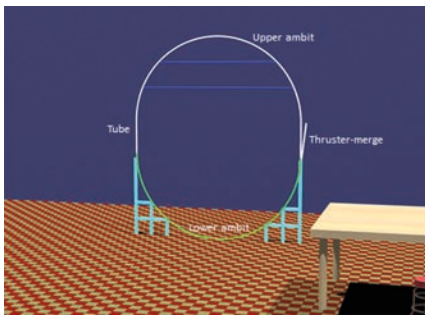


Fig.3 Four-metre-high prototype.

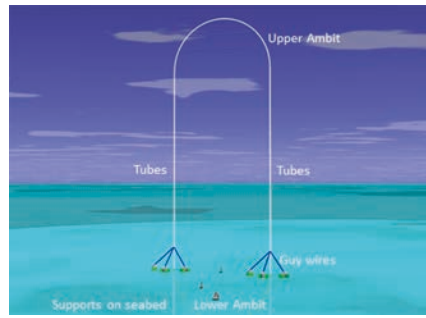


Fig.4 Mile-high tower.



Fig.5 Preliminary construction at sea.

Thailand is shown in Fig. 5, but unfortunately it had to be abandoned owing to licensing problems.

Detailed simulations have been performed of all the components of the four-metre-high prototype and the ambits of the mile-high tower. The Radia 3-D magnetostatics package was used with additional code to add dynamic capability.[10] Two versions of the ambits were simulated, one using permanent neodymium-iron-boron (NIB) magnets with electromagnets to provide stabilization, and the other using high-temperature superconductors (HTS). The HTS used in the initial construction and testing was Yttrium Barium Copper Oxide (YBCO), which requires temperatures below 80 K for which we used liquid nitrogen.

To minimize eddy currents, needle NIB magnets bound together with insulating material are proposed for the mile-high tower, as shown in Fig. 6. This only reduces the magnetic field strength by about 2%, but is expected to eliminate all but the tiniest eddy currents. However, ordinary NIB magnets were used for the prototyping work in the arrangement shown in Fig. 7. Each bolt (in green) consists of a pair of half-Halbach arrays which match similar arrays on each side along the ambit. The electromagnets are above and below the bolts. In the four-metre-high prototype, the bolts travel at 45 m/s and the ambit radius is 1.5 m. In the mile-high tower, the bolts travel at 360 m/s and the ambit radius is 45 m.

A key issue outside the controlled environment of a workshop is stability in the presence of gusting winds. A mathematical proof of stability has been published, but the design details

now available together with some detailed simulations show the need for an update. In particular, the stiffness of the tubes complicates the behaviour.

The basic equation governing the motion of the tubes is:

$$m_b \left( \frac{\partial^2 z_b}{\partial t^2} + 2v \frac{\partial^2 z_b}{\partial t \partial x} + v^2 \frac{\partial^2 z_b}{\partial x^2} \right) - w = R_e + m_t \frac{\partial^2 z_t}{\partial t^2} + T \frac{\partial^2 z_t}{\partial x^2} - EI \frac{\partial^4 z_t}{\partial x^4} \quad (1)$$

Here  $z_b$  and  $z_t$  are the lateral displacements of the stream of bolts and the tube, respectively. We consider one dimension but the same analysis applies to the orthogonal dimension. They are functions of time  $t$  and distance  $x$  along the tube. The bolts travel along the tube at velocity  $v$ . The mass of a stream of bolts per metre is  $m_b$  and the tube's mass per metre is  $m_t$ .  $T$  is the tension in the tube. We take  $m_b$ ,  $v$ ,  $T$  and  $m_t$  as constant, although they do vary slowly with distance along the tube; the bolts slow down and become closer as they ascend and speed up as they descend. The term in  $EI$  is due to the stiffness and was not present in the earlier analysis.  $E$  is Young's modulus and  $I$  is the second moment of area of the tube. The wind force is  $w$ , and there is an internally generated force  $R_e$  to control the bending. We define it as follows:

$$R_e = R_c + m_b \frac{\partial^2 z_r}{\partial t^2} + 2m_b v \frac{\partial^2 z_r}{\partial t \partial x} + m_b v^2 \frac{\partial^2 z_r}{\partial x^2} \quad (2)$$

$R_e$ ,  $R_c$  and  $w$  are per metre. This definition introduces the required displacement  $z_r$  of the tube and bolts from a straight line in order to provide the curvature  $c_r = \frac{\partial^2 z_r}{\partial x^2}$  required so that the centrifugal force as the bolts travel round it will match the wind force  $w$ .  $R_c$  is derived from the bending compensation  $B_c$ .

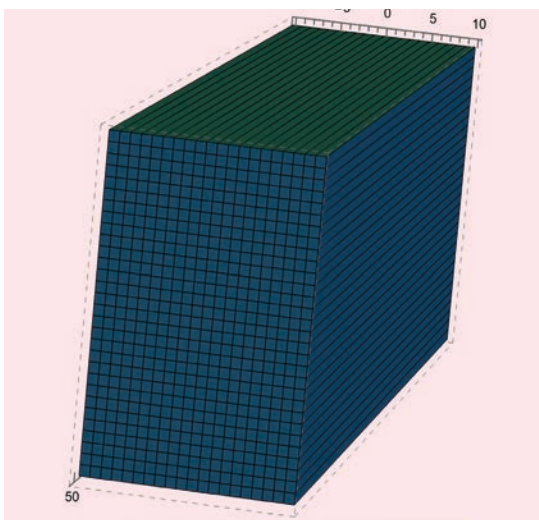


Fig.6 Bolt composed of needle magnets to avoid eddy currents.

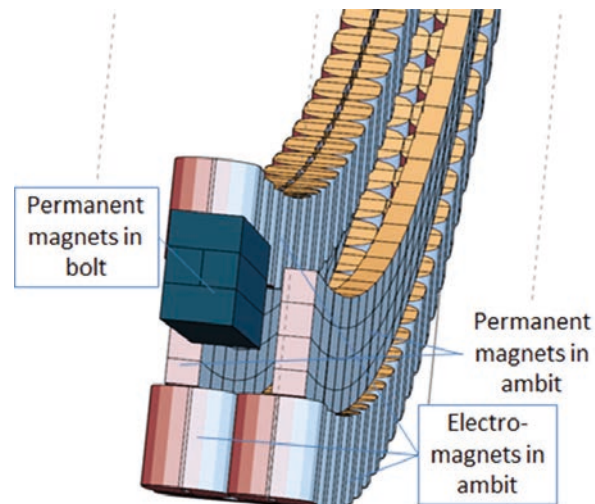


Fig.7 Simulation of a bolt in the lower ambit.

$$R_c = \iint B_c dx dx \tag{3}$$

$$B_c = \chi \frac{\partial^2}{\partial x \partial t} (c - c_r) + \xi \frac{\partial^2}{\partial x^2} (c - c_r) - \epsilon (c - c_r) - \kappa \frac{\partial}{\partial t} (c - c_r) \tag{4}$$

Here  $c_r = \frac{\partial^2 z_r}{\partial x^2}$ . This definition is designed to coerce the tube and the stream of bolts to conform to the required curvature  $c_r$ . The coercive term is in the constant  $\epsilon$ ; the term in the constant  $\kappa$  provides damping; and the terms in the constants  $\chi$  and  $\xi$  deal with wind shear and its derivatives. The publications cited contain a lengthy derivation of the constraints on the constants using the Laplace transform.

The required curvature and displacement are derived from equation (1) by seeking a stable position in which the time derivatives are zero,  $R_e = 0$ , and  $Z_b = Z_t = Z_r$  as follows:

$$m_b v^2 \frac{\partial^2 z_r}{\partial x^2} - w = T \frac{\partial^2 z_r}{\partial x^2} - EI \frac{\partial^4 z_r}{\partial x^4} \tag{5}$$

Assuming  $z_r = 0$  and  $\frac{\partial z_r}{\partial x} = 0$  at  $x = 0$ , and  $z_r = Z_L$  and  $\frac{\partial z_r}{\partial x} = D_L$  at  $x = L$ , the solution is:

$$z_r = \frac{1}{a^2} (P(1 - \cos ax) + Q(ax - \sin ax)) + \frac{1}{2} \frac{w x^2}{m_b v^2 - T} \tag{6}$$

Here

$$a = \pm \sqrt{\frac{m_b v^2 - T}{EI}} \tag{7}$$

$$P = w \frac{aL \cot aL + 2 - aL \csc aL}{2(m_b v^2 - T)} - \frac{aZ_L}{L} (\cot aL + \csc aL) - \frac{D_L}{L} (1 - aL \csc aL) \tag{8}$$

and

$$Q = 2 \frac{2 \cot aL - 2 \csc aL - aL}{2(m_b v^2 - T)} + \frac{aZ_L}{L} + \frac{D_L}{L} (\csc aL - \cot aL) \tag{9}$$

The approach being taken is to apply the bending compensation at selected points A,B,C,D,... at equal intervals spaced a distance  $l$  apart along the tube, as in Fig. 8.

### 3 INTERPLANETARY TRAVEL

Once a space elevator has been constructed, it will open up many opportunities that are not available today. The point at the furthest end of the tether, known as the apex anchor, rotates with the earth at the same angular velocity of  $7.29 \times 10^{-5}$  rad/s. At the earth's equator the velocity is 465 m/s in the easterly direction. At the geosynchronous altitude (GEO at 35,786 km) the velocity is 3.1 km/s, the velocity of geosynchronous

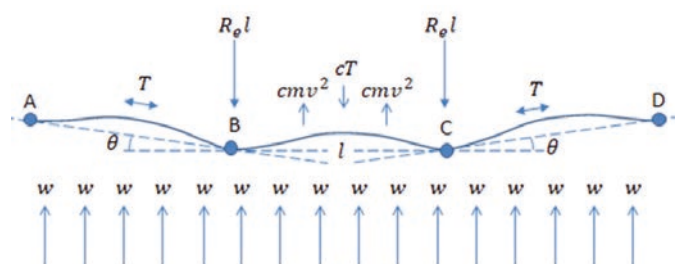


Fig.8 Bending control points.

orbit. At 100,000km the velocity is 7.6 km/s, which is above the Earth's escape velocity there. Consequently interplanetary vehicles can be launched there with little fuel required[11]. Mars can be reached in just 60 days [12].

Vehicles require power to be supplied to them as they ascend to GEO, but beyond that point they naturally accelerate due to the centrifugal force of rotation about the earth, which is stronger than the centripetal force of gravity beyond GEO. The energy and momentum needed are supplied from the Earth's rotation, although the impact to the Earth is many orders of magnitude less than the daily effect of the tides. To enable vehicles to arrive at the apex anchor at a moderate speed, braking will be needed. However, a radical proposal is to allow vehicles to accelerate naturally beyond GEO [13]. Then they arrive at the apex anchor travelling away from the earth at 10 km/s, and this is additional to the velocity in the orbital direction of 7.6 km/s. To gain maximum benefit, Peet proposes that a steerable ramp is provided at the apex anchor to direct this velocity towards the desired destination in the solar system or beyond.

Using this method, journeys throughout the solar system are feasible at very moderate expense and in short transit times, e.g., Jupiter 450 to 850 days, and Neptune in 4,000 to 4,365 days. In addition, missions to the Oort cloud and the heliopause will be much easier than now. Fuel will be needed only for course correction and deceleration. It will be feasible to make such journeys often and at modest cost.

Another method has been proposed that avoids the need to move vehicles at high speed along the tether. This is the method known as secondary tethers.[14] It gives spacecraft a gentle ride, never subjecting them to more than a g-force of one, i.e., the force of gravity on the Earth, approximately equivalent to an acceleration of 10 m/s<sup>2</sup>.

In the standard model of a space elevator, a mass of 1,900 tonnes is needed at the apex anchor to balance the other forces in the tether.[2] It may comprise discarded construction machines and material. This mass depends on the distance from the Earth. It reduces as we go outwards, vanishing if we make the tether 150,328 km long [15]. The method of secondary tethers requires a mass at the apex anchor of 2,272 tonnes, assuming a requirement to launch spacecraft of up to 16 tonnes mass. Shortening the primary tether (i.e., the tether from the Earth's surface) from 100,000 km to 90,000 km is one way to achieve the desired result, but it is simpler to thicken the primary tether in proportion, since it scales linearly in proportion to the maximum load[16]. It is similarly possible to scale up the secondary tethers to accommodate bigger spacecraft.

We assume that the multi-stage approach is not needed and the secondary tethers are made of graphene super laminate; they are arranged in two counter-rotating sets of three as in Fig. 9. They rotate about the axis of the primary tether, which itself rotates about the earth, of course. Thus over the course of a day it is easy to launch in any direction.

The space elevator's primary tether rotates in the earth's equatorial plane (Fig. 10). Consequently any spacecraft that is released directly from the primary tether will remain in the equatorial plane. The solar system is inclined at 23.45° from the ecliptic, although there are variations. A second plane is needed, by analogy with longitude and latitude on the earth. Then we can specify the direction to any destination in the universe. A release point on the equator gives selection of a

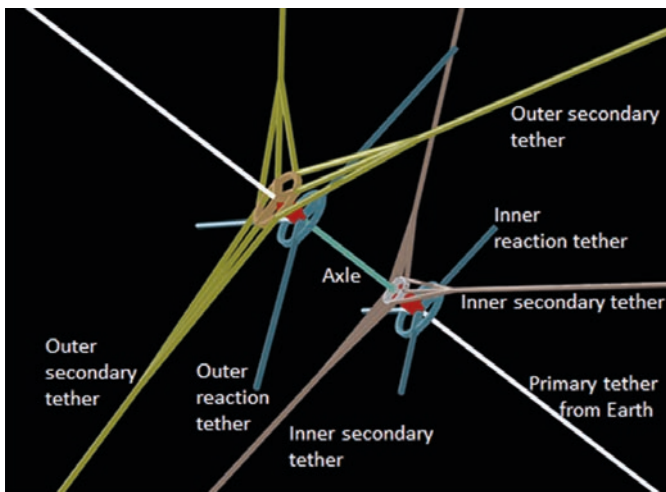


Fig.9 Secondary tethers with reaction wheels, axle and primary tether.

particular longitude; the secondary tethers give an analogous selection of a particular latitude. Astronomers use declension and right ascension on the notional celestial sphere instead, but the principle of needing two angles to specify any direction is the same.

The velocity at the end of a secondary tether is 10 km/s, to which can be added the 7.6 km/s due to the earth's rotation. Depending on the timing of its release, the spacecraft can be launched in any direction on the celestial sphere. In especially favourable situations, the maximum of 17.6 km/s can be achieved, but usually the vector sum at the desired angles will be less. The minimum is the square root of the sum of the squares, which is 12.6 km/s.

The analysis takes account of the gyroscopic effects as well as the centrifugal forces due to rotation about the axis and about the earth. The reaction wheels are required to balance the gyroscopic forces caused by the rotation of the secondary tethers about the axle while they are also rotating about the earth. The outer secondary tethers are each 10,000 km long and rotate at an angular velocity of  $10^{-3}$  radians/s, thus making the velocity at the end 10 km/s. Spacecraft are launched from one of these three outer secondary tethers. The outer reaction tethers are 20 km long and rotate at 1 radian/s. They match the gyroscopic forces but not the angular momentum. As the outer secondary tethers vary their angular momentum, the inner secondary tethers must perform an equal and opposite variation. The axle is required to transmit these changes in momentum, which are due to startup and launch operations. Its length is 4.3 km, which is enough to avoid collisions between the inner and outer secondary tethers. The axle deals with rotations and transmits torque, but it does not tolerate large bending moments. It has a novel design made of graphene wrapped round a core of Dyneema.

The inner secondary tethers are 1,100 km long and rotate at 0.0308 radians/s. The inner reaction tethers are 8 km long and rotate at 1 radian/s. The inner reaction tethers match the gyroscopic forces on the inner secondary tethers. The inner combination of secondary tethers and reaction tethers together balance the rotational momentum of the outer combination of secondary and reaction tethers. Between the secondary tethers and their reaction tethers are strong connectors 3 m long that can take bending moments amounting to  $1.1 \times 10^8$  Nm due to the gyroscopic forces.

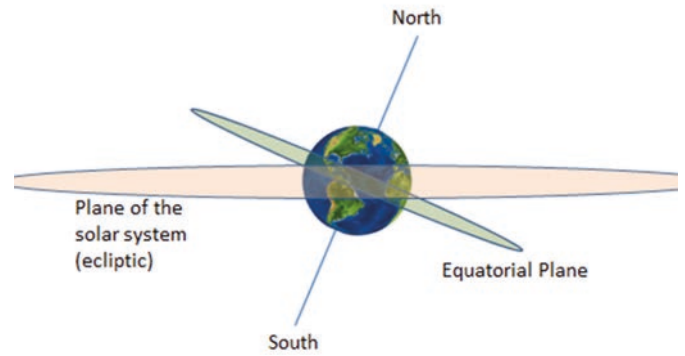


Fig.10 Plane of the equator and the ecliptic.

Fig. 11 shows the gyroscopic and other effects. The 4.3 km axle can be seen connecting the outer and inner secondary tethers. Just visible are the reaction tethers immediately to the right of the secondary tethers with strong 3 m connectors. The gyroscopic forces are calculated using Euler's equations of rotational motion, of which the critical one is:

$$-(C - A)\omega_3\omega_1 = G_2 \tag{10}$$

Here  $\omega_1 = 10^{-3}$  radians/s is the outer secondary tethers' angular velocity about the axle,  $\omega_3 = 7.29 \times 10^{-5}$  radian/s is their angular velocity about the Earth,  $C$  and  $A$  are the moments of inertia about these same axes, and  $G_2$  is the resultant couple. The tethers are not rigid bodies, and so the forces are calculated on short segments. The moment of inertia about the axle of a segment of mass  $m_s$  at a distance  $d$  from the axle is  $A = m_s d^2$ . The value of  $C$  is very small. The net gyroscopic force on a segment is  $F_G = G_2/d = m_s d \omega_3 \omega_1$ . In addition there are centrifugal forces  $F_C = m_s d \omega_1^2$  about the axle and  $F_E = m_s \sqrt{D^2 + d^2} \omega_3^2$  about the Earth, where  $D$  is the distance from the Earth's centre. The resolution of these forces gives an accumulated couple on the strong connector of  $1.1 \times 10^8$  Nm. This is balanced by an equal and opposite couple from the reaction tethers. The combined effect is illustrated in Fig. 11. The force  $F_C$  pulls them away from the axle, but the centrifugal force about the Earth pulls them away from the Earth. The gyroscopic force rotates

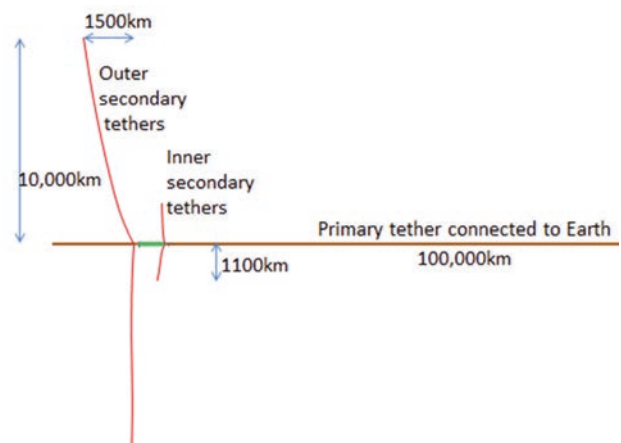


Fig.11 View of secondary and reaction tethers showing displacements.

them about the third axis, which is orthogonal to the other two. It pulls them away from Earth during one half of their rotation about the axle and towards Earth for the other half. For half their rotation the forces reinforce each other, and for the other half they almost cancel out. The combined effect is that the maximum displacement from the plane is 1,500 km. This is the displacement from the plane in which they would rotate if they were not also rotating about the Earth.

The same formulae apply to the inner secondary tethers and the reaction tethers, but the numbers are very different. The reaction tethers are displaced from the plane by a maximum of only 2.5 m, and so the strong connectors only need to be 3 m long. Since they rotate in the opposite direction to the secondary tethers, their gyroscopic tilt is opposite to that of their secondary tethers. The inner secondary tethers also counter-rotate with respect to the outer ones, and so their tilts are opposite. The inner secondary tethers are needed because the reaction tethers do not match the angular momentum of their secondary tethers. The numbers are  $10^{15}$  kg.m<sup>2</sup>/s compared to  $4 \times 10^{12}$  kg.m<sup>2</sup>/s. The inner secondary tethers are optimized to keep the axle as short as possible; their displacement away from the plane is only 4.3 km, and so this is the length of the axle. They then need their own set of reaction tethers to balance their gyroscopic forces.

### 3.1 Launching spacecraft and recoil

Spacecraft will travel along one of the outer secondary tethers at moderate speed powered by the centrifugal force due to rotation about the axle. The spacecraft is released at the time of day and the time of its rotation about the axle chosen so that it travels in the required direction. It is possible to slow or speed up the rotation of the secondary tethers to give the exact timing required (see Ref. [14]).

A problem identified in Ref. [14] is maintaining balance and stability when a spacecraft is released. Just before its release, the centre of gravity of the set of secondary tethers would be displaced from the axle by  $d \frac{m_p}{M_o} \approx 200$  km, where  $d = 10,000$  km is the distance from the axle to the end of the tether,  $m_p = 16$  tonnes is the mass of the spacecraft, and  $M_o = 800$  tonnes is the mass of the outer secondary tethers with their reaction tethers, wheels and drive mechanism. To avoid this problem, the other two secondary tethers will simultaneously need to release a load of ballast equal in mass to that of the spacecraft.

Another approach would be to have four secondary tethers instead of three. Then only one secondary tether would need to release ballast instead of two. There is a trade-off to be made.

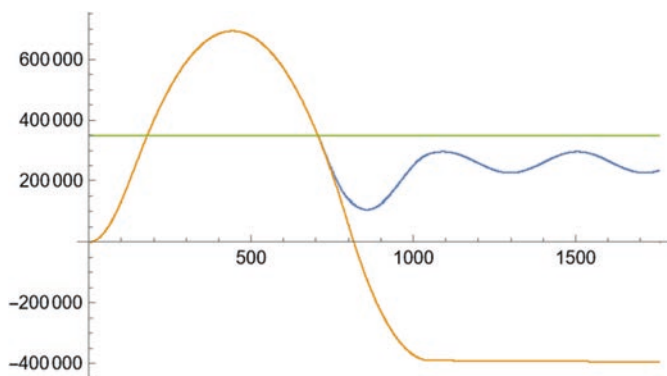


Fig.12 Movement of the stabilizers in metres vs. seconds.

Another question to deal with is the effect of releasing the spacecraft or ballast on the secondary tethers, which will be under tension. The release will cause them to start moving inwards towards the axle. Eventually the centrifugal force will restore them to their correct position. The release will cause a reduction in tension of  $T_s = 160$  kN along the length  $L = 10^7$  m of the tether, leading to a contraction of  $\frac{T_s L}{EA} \approx 348$  km, where  $E = 10^{12}$  is the Young's modulus of graphene and  $A = 2.16 \times 10^{-6}$  is the area of cross section. At the end  $A = 2.16 \times 10^{-6}$  m<sup>2</sup>, but it varies along the length, and so the spreadsheet was used to calculate the contraction. To avoid undesirable whiplash effects on the secondary tethers, we hold a mass of 4 tonnes at the end of each one. These masses are called *stabilizers*; they are permanently present to reduce the effect of the jerk. When a spacecraft (or ballast) departs, the stabilizers will move towards the axle a distance of 700 km and will oscillate about the new stable point, i.e., the point 348 km from where they were when the spacecraft was released.

To control the oscillation, the stabilizers are designed to split into two equal parts. The outer stabilizer is allowed to move outwards much further than the inner stabilizer so that it can be used to dampen the oscillation. The two parts are held together by a connecting tether that unrolls and rolls up as required to maintain the necessary tension.

The movement is shown in Fig. 12. The horizontal line is the new stable position (348 km) after the spacecraft has departed. As the diagrams show, the mechanism separates the stabilizers after 707 seconds. The inner one moves with reduced oscillations towards the stable position and the outer one (below it) reaches a temporary stable distance 389 km further out from the origin, where it can be pulled in under control. The velocities are in Fig. 13. More than one such manoeuvre may be needed to complete the stabilization process.

The motion of the stabilizers when under tension from the secondary tether satisfies the following equation:

$$m \frac{d^2 x}{dt^2} = T \left( 1 - \frac{x}{D} \right) - C \tag{11}$$

Here  $x$  is the displacement towards the axle from the starting point at which the spacecraft is released, which is the origin,  $t$  is time,  $m$  is the mass of the stabilizers,  $T$  is the tension at the end of the secondary tethers,  $D = 348 \times 10^3$  m is the distance from the origin to the new stable position, and  $C$  is the centrifugal force due to the rotation about the axle. We have taken the approximation that  $C$  is constant, because it varies much more slowly than the tension. Also, we have used point

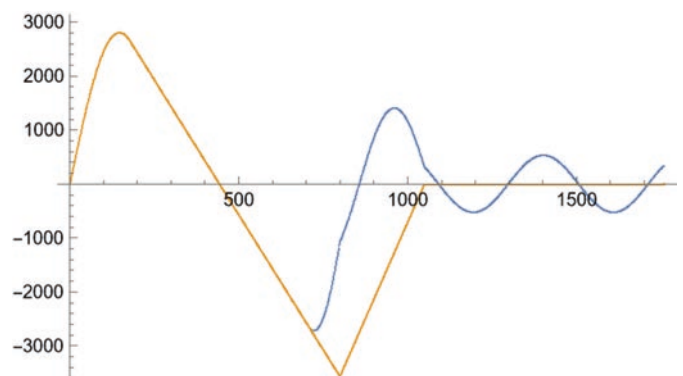


Fig.13 Velocities of the stabilizers in m/s vs. seconds.

masses to include approximations to the distributed masses of the tethers. The connecting tether has a mass of 800 kg which will have a varying distribution depending on the separation between the two stabilizers. A full analysis would need to take this into account.

When a stabilizer passes the new stable position at 348 km from the origin, it is no longer subject to tension and its equation of motion is simply:

$$m \frac{d^2 x}{dt^2} = -C \tag{12}$$

The respective solutions of these equations are:

$$x = P \cos kt + Q \sin kt + D \left( 1 - \frac{C}{T} \right) \tag{13}$$

$$x = x_1 + \left( v_1 + \frac{C t_1}{m} \right) (t - t_1) - \frac{C}{2m} (t^2 - t_1^2) \tag{14}$$

Here  $k^2 = T/mD$ ,  $x_1$  is the starting position at which the equation applies,  $v_1$  is the starting velocity,  $t_1$  is the starting time, and  $P$  and  $Q$  satisfy:

$$P = D \frac{C}{T} \cos kt_1 - \frac{v_1}{k} \sin kt_1 \tag{15}$$

$$Q = D \frac{C}{T} \sin kt_1 + \frac{v_1}{k} \cos kt_1 \tag{16}$$

Equations (11) and (13) with  $x_1 = 0 = v_1$  apply initially. After seconds, equations (12) and (14) apply with  $x_1 = D$ ,  $t_1 = 180$  seconds, and  $v_1 = 2,630$  m/s. The stabilizers cross the stable position again at  $t = 707$  seconds with a similar but opposite velocity of  $-2,640$  m/s.

The oscillations would continue for a very long time without some way of damping the motion. The technique chosen is to separate the two stabilizers at this point. The inner stabilizer remains attached to the secondary tether which retards its motion following equations (11) and (13) but with  $m = 2,000$  kg instead of 4,000 kg. The outer stabilizer is still subject to equations (12) and (14) but with  $m = 2,000$  kg; it continues and in fact accelerates due to the centrifugal force. As the two stabilizers separate, the tether connecting them has to unroll freely until a critical point is reached when a brake is applied on the connecting tether's roll. The tension thus caused slows the outer stabilizer while also damping the motion of the inner stabilizer. The chosen regime is to apply a force of 40 kN for 250 seconds from  $t = 800$  to  $t = 1,050$  and then to apply a small force that just overcomes the centrifugal force and so causes the two stabilizers to reunite over a period of hours with minimal oscillation. In equations (11) to (14), these additional forces simply appear as an altered value of  $C$ .

This regime may not be optimal; the point here is to show that such a regime exists. As the graphs show, the inner stabilizer oscillates below the stable distance towards which it will gradually move while at the same time slowly tugging the outer stabilizer towards itself.

### 3.2 Other issues affecting stability

Further work is needed to examine the behaviour of the reaction tethers when a spacecraft is released. In addition, a

mechanism is needed for spacecraft to pass through the inner secondary tethers on their way to the outer secondary tethers, probably by making the strong connectors into tubes that are wide enough to accommodate a spacecraft inside them and devising a lock mechanism to maintain contact with the primary tether.

Because the space elevator will provide low-cost access, it will be possible to experiment on a small scale at the apex anchor before attempting to build the full-size version.

## 4 GEOSYNCHRONOUS ALTITUDE

Whereas at the apex anchor care must be taken to maintain the overall balance of the tether, at GEO there are no such constraints. If a space elevator has a daily lifting capacity of 14 tonnes of payload, over 10 years it can lift 42,000 tonnes to GEO, assuming 300 days of productive service a year. By comparison, the international space station has a mass of 420 tonnes and accommodates seven people who conduct many experiments and tasks, particularly those associated with microgravity. A single space elevator can lift 420 tonnes in only 30 days, and so many microgravity facilities can be developed there. If greater capacity is required, the tether can be thickened in proportion to the payload desired. More than one space elevator will be built to increase the lifting capacity further and to make it easy to recover if one should ever fail.

The applications include communications, broadcast and earth observation, as with present-day satellites in orbit now. Astronomy and other scientific work will blossom and flourish there. Grand projects such as launching interstellar probes will be possible at reasonable cost. Space-based solar power will be very attractive financially as well as benefiting the earth's environment.

From the tether at GEO, a station can be built that extends in the three orthogonal directions, as in Fig. 14.

1. The orbital direction east and west, although this is a crowded orbit
2. The north-south direction
3. Away from or towards the Earth

Extending in the orbital direction east-west is the simplest approach but is limited by the crowded nature of the orbit. However, over the middle of the Pacific Ocean there is plenty of room. A space elevator anchored in the central Pacific would be ideal for constructing a large spaceship such as a generation starship that would be built over a period of years and then dispatched on an interstellar journey. Even in the regions due south of the US, Europe and East Asia most of the satellites,

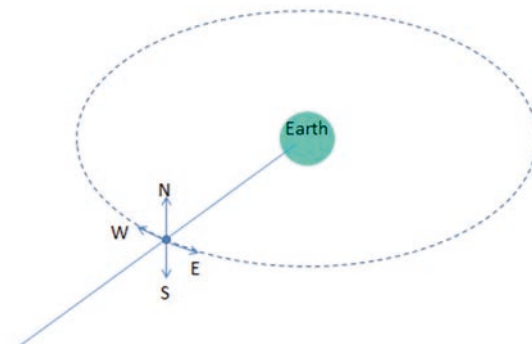


Fig.14 The three orthogonal directions from a space elevator at GEO.

with some exceptions, are spaced at least one degree of longitude apart. Since the length of the orbit is 265,000 km, one degree is 736 km, so there is room for quite large structures even there.

Extending in the other two orthogonal directions is wide open and there is unoccupied space there. It will require a balance to be maintained. An extension to the north will require an equal extension to the south. The result will be a tiny force of gravity on the north extension pulling it back towards the mid-point and an opposite force on the south extension. The acceleration due to gravity that causes this force will be  $g \sin \theta$ , where  $g = 0.224 \text{ m/s}^2$  is the acceleration due to gravity at GEO and  $\sin \theta = l/D$ .  $D = 42170 \text{ km}$  and  $l$  is the distance of the centre of gravity of the extension from the mid-point. If  $l = 100 \text{ m}$  then  $g \sin \theta = 0.224 \times 100/4.217 \times 10^7$ , which is  $5.3 \times 10^{-7} \text{ m/s}^2$ . If the extension has a mass of 1,000 tonnes, the force directed towards the mid-point will be 530 mN, a truly tiny amount. The structure needed to support it will be very slender. Even if  $l = 100 \text{ km}$ , the force is just 530 N, about 54 kg weight, still a small compressive force.

An extension in the direction away from the Earth will be subject to a reduction of gravity and an increase in centrifugal force that will tend to pull it further away. Similarly, an extension towards the Earth will experience somewhat greater gravity than the centrifugal force and so will tend to drift towards the earth. The two can be balanced if connected to the mid-point by a simple arrangement of tethers to hold them in place.

The acceleration  $g$  due to gravity at a distance  $h$  above the mid-point (i.e., in the direction away from the Earth) is reduced by a factor  $D^2/(D+h)^2$ , and so the acceleration reduction is  $g[1 - D^2/(D+h)^2]$ .

If  $h = 100 \text{ m}$  above the mid-point, this comes to  $0.224 \times 4.74 \times 10^{-6} = 1.06 \times 10^{-6} \text{ m/s}^2$ . There is an increase in the acceleration  $c$  due to the centrifugal force of rotation about the Earth. It increases linearly with distance, so the increase is  $ch/D$ . Since  $c = g$  by the nature of GEO, the change is  $5.3 \times 10^{-7} \text{ m/s}^2$ . Hence the net acceleration is the sum of these two, which amounts to  $1.59 \times 10^{-6} \text{ m/s}^2$ . The force on a 1,000 tonne extension is therefore 550 mN, a trivial amount.

Even for a 1,000 tonne extension 1,000 km above the mid-point, the equivalent calculation yields a force of 15.5 kN, equivalent to just 1.6 tonnes weight. The balancing extension should be 950 km below and also 1,000 tonnes, although these parameters can be varied as long as the balance is maintained.

Of course, provision must be made for climbers on the tether to pass through above and below without being impeded.

## 5 CONCLUSIONS

The emergence of graphene super laminate once more illustrates the extraordinary properties of carbon in its many forms. Although it is not yet available in the quantities required for space elevators, the way that industry is gearing up is very promising. Hexagonal Boron Nitride is another 2D material that meets the requirements and should not be overlooked.

Augmenting the space elevator with dynamically supported structures will permit space elevators to be built with weaker materials than with the standard model, but it does increase the complexity of the project. Lofstrom's original proposal for the Launch Loop was intended to launch spacecraft directly to orbit, and the Space Cable was proposed for single-stage-to-orbit spacecraft by raising and accelerating 90 tonne spacecraft to 5,000 km/h at 50 km altitude, effectively replacing the first stage rocket. Developing the base technology will enable other applications, such as emergency platforms for tall buildings, solar panels above the clouds, and providing augmented take-off for terrestrial travel with rocket planes and scramjets [17].

The extraordinary possibilities at the apex anchor continue to unfold as more opportunities come to be understood. Without the use of fuel or the need for spacecraft to carry reaction mass, the solar system and near-interstellar space can be explored at will without having to wait a long time for planetary alignments and gravity-assist manoeuvres. Furthermore, the gentle launch method removes the need for complicated measures to make delicate payloads robust; they will not need to withstand the forces of a rocket blasting off. The costs will be much lower than today, which means that it will be possible to improve reliability of missions by launching duplicate or triplicate probes at very moderate costs.

The opportunities to build near GEO are huge. Building towards the earth will make it possible to have geosynchronous installations nearer to the Earth than the usual 35,786 km; it looks like an attractive position for space-based solar power. Building north or south also presents practically unlimited possibilities while still maintaining quite a small footprint in the geostationary orbit itself.

There are other projects underway or recently completed, including work on tether simulators and on the interface between the tether and the climbers, which have to deal with the low friction of graphene [18].

## REFERENCES

1. A. Nixon, J. M. Knapman, D. H. Wright, "Space Elevator Tether Materials: an Overview of the Current Candidates", *Acta Astronautica*, Vol. 210, pp. 483-487 (2023)
2. P. A. Swan, D. I. Raitt, C. Swan, R. E. Penny, J. M. Knapman, "Space Elevators: an Assessment of the Technological Feasibility and the Way Forward", *International Academy of Astronautics, Paris, 2013*
3. J. S. Lee, S. H. Choi, S. J. Yun, Y. I. Kim, S. Boandoh, J-H. Park, B. G. Shin, H. Ko, S. H. Lee, Y-M. Kim, Y. H. Lee, K. K. Kim, S. M. Kim, "Wafer-scale Single-crystal Hexagonal Boron Nitride Film Via Self-collimated Grain Formation", *Science*, Vol 362, Issue 6416, pp. 817-821
4. Y. Bai, R. Zhang, X. Ye, Z. Zhu, H. Xie, B. Shen, D. Cai, B. Liu, C. Zhang, Z. Jia, S. Zhang, X. Li, F. Wei, "Carbon Nanotube Bundles With Tensile Strength Over 80 GPa", *Nature Nanotechnology*, 13, pp. 589-595 (2018)
5. B. Quine, US Patent no. 9085897 "Space Elevator" granted 21 July 2015
6. K. Lofstrom, "The Launch Loop", *AIAA Paper 85-1368*, July 1985
7. J. M. Knapman, "The Space Cable: Capability and Stability", *JBIS*, 62, No.6, pp. 202-210 (2009)
8. J. M. Knapman, "Active Curvature Control for the Multi-stage Space Elevator", *73rd International Astronautical Congress, Paris, France, September 18-22, 2022*
9. J. M. Knapman, P. Glaskowsky, D. Gleeson, V. Hall, D. Wright, M. Fitzgerald, P. A. Swan, "Design Considerations for the Multi-stage Space Elevator", *ISEC position paper 2019-1*, International Space Elevator Consortium, February 2019
10. O. Chubar, P. Elleaume, J. Chavanne, "A 3D Magnetostatics Computer



- Code for Insertion Devices”, *J. Synchrotron Rad.* (1998) 5, pp.481-484.
11. B.C. Edwards, P. Ragan, *Leaving the Planet by Space Elevator*, lulu.com, 2006
  12. J. Torla, M. Peet, “Optimization of Low Fuel and Time-critical Interplanetary Transfers Using Space Elevator Apex Anchor Release: Mars, Jupiter and Saturn”, *70th International Astronautical Congress, Washington, D.C., USA, 2019, 21-25 October*.
  13. M. Peet, “The orbital mechanics of space elevator launch systems”, *Acta Astronautica*, **179** pp. 153-171 (2021)
  14. J. M. Knapman, P. A. Swan, “Secondary Tethers”, *Acta Astronautica*, **195**, pp. 561-566 (2022)
  15. J. Pearson, “The Orbital Tower: a Spacecraft Launcher Using the Earth’s Rotational Energy”, *Acta Astronautica*, **2**, pp. 785-799 (1975)
  16. B. Shelef, “The Space Elevator Feasibility Condition,” *Climb*, Vol.1, No.1, p.87, The International Space Elevator Consortium, 2011
  17. J. Knapman, “Diverse Configurations of the Space Cable,” *61st International Astronautical Congress, Prague, Czech Republic, September 27-October 1, 2010*
  18. D. H. Wright, L. Bartoszek, A. J. Burke, D. Dotson, H. El Chab, J. M. Knapman, M. Lades, A. Nixon, P.W. Phister Jr., P. Robinson, “Conditions at the Interface Between the Space Elevator Tether and its Climber”, *Acta Astronautica* online 28th June, 2023
- 

**Received 23 August 2023 Approved 28 September 2023**